JCEC
THE JOURNAL OF ENGINEERING AND EXACT SCIENCES

OPEN ACCESS

The Journal of Engineering and Exact Sciences – jCEC, Vol. 10 N. 04 (2024)
journal homepage: https://periodicos.ufv.br/jcec
eISSN: 2527-1075
ISSN: 2446-9416

Comparative analysis of harmonic sensitivity for stator fault diagnosis in induction motors

Article Info:
Article history: Received 2023-09-03 / Accepted 2024-01-20 / Available online 2024-01-30
doi: 10.18540/jcecvl10iss4pp18212

Allal Abderrahim
ORCID: https://orcid.org/0000-0002-7382-5180
Faculty of Technology, University of El-Oued, 3900 El Oued, Algeria
E-mail: allalabderrahim@yahoo.fr
Lamouchi Zakaria
ORCID: https://orcid.org/0000-0003-2240-3540
Faculty of Technology, University of El-Oued, 3900 El Oued, Algeria
E-mail: prof_lammouchi@yahoo.fr
Khechekhouche Abderrahmane
ORCID: https://orcid.org/0000-0002-7278-2625
Faculty of Technology, University of El-Oued, 3900 El Oued, Algeria
E-mail: abder03@hotmail.com
Antonio Marcos de OliveiraSiqueira
ORCID: https://orcid.org/0000-0001-9334-0394
Universidade Federal de Viçosa, Brazil
E-mail: antonio.siqueira@ufv.br
Julio César Costa Campos
ORCID: https://orcid.org/0000-0002-9488-8164
Universidade Federal de Viçosa, Brazil
E-mail: julio.campos@ufv.br
Kheireddine Lamamra
ORCID: https://orcid.org/0000-0002-9867-8463
Laboratory LENT, University of Oum El Bouaghi, Algeria
E-mail: lamamra.kheireddine@univ-oeb.dz

Abstract
Induction motors play a vital role in various industrial applications due to their commendable efficiency and reliability. However, their susceptibility to faults, especially in challenging industrial environments, highlights the need for vigilant fault detection to prevent unforeseen downtimes and reduce subsequent repair costs. Early fault diagnosis is crucial in this context. A systematic approach to diagnosing faults in asynchronous motors involves the application of signal processing techniques, particularly utilizing the Fast Fourier Transform (FFT). The FFT, as a mathematical tool, enables a comprehensive analysis of signals, facilitating the identification and isolation of their frequency components. Monitoring the frequency components within a motor's signal provides a means to determine the existence and severity of faults. FFT analysis allows for the monitoring of four distinct categories of harmonics: time harmonics (TH), rotor slot harmonics (RSH), rotor bar fault harmonics (RBFH), and eccentricity fault harmonics (EFH). Each type of harmonic offers valuable insights into specific fault categories. Empirical evidence, drawn from experimental results, emphasizes the heightened sensitivity of rotor slot harmonics (RSH) in detecting stator faults. Continuous monitoring of the RSH frequency component enables the prompt detection and localization of stator faults, along with an assessment of their severity. Additionally, this diagnostic methodology proves effective in identifying micro short-circuits between stator coils, allowing for

a proactive strategy in predictive maintenance. This proactive approach enables anticipatory part replacement before degradation progresses to the point of causing comprehensive failure in the production chain. The combination of FFT-based signal processing and harmonic analysis establishes a robust framework for the early detection and localization of faults in asynchronous motors within industrial settings. This contributes to enhanced operational reliability and efficiency, ultimately ensuring smoother industrial processes.
Keywords: Inter-Turns. Motor induction. FFT. Time harmonics. Slots rotor harmonics. Eccentricity fault harmonics. Rotor bar fault harmonics.

1. Introduction

Diagnosis plays a pivotal role in ensuring the reliability, safety, and efficiency of electric power systems. Timely identification and resolution of issues contribute to minimizing outage impact, reducing costs, and enhancing overall grid performance. Research efforts, particularly in engineering, have been dedicated to advancing diagnostic tools and techniques. Notably, the exploration of sophisticated diagnostic methods, including the application of machine learning algorithms such as Artificial Neural Networks (ANNs) and Support Vector Machines (SVMs), has gained substantial attention for analyzing extensive datasets and identifying patterns indicative of faults or anomalies (Almounajjed *et al.*, 2022; Bilal Djamal Eddine *et al.*, 2020; Cherif *et al.*, 2020; Senthil Kumar *et al..*, 2022; Tian *et al.*, 2022).

Consideration of harmonics in the Finite Element Method (FMM) and flux density distribution is crucial. Advanced modeling techniques incorporating harmonic effects, alongside diagnostic tools capable of detecting and analyzing these harmonics, enhance the accuracy of results and improve the real-world performance and reliability of squirrel-cage induction motors (Abdelhak *et al.*, 2022; Boucherma *et al.*, 2006; Devanneaux *et al.*, 2003; Năvrăpescu *et al.*, 2010; Saad *et al.*, 2014)

The Harmonic Phase Vector Pattern Analysis (HPVPA) technique, employed for condition monitoring and fault diagnosis of rotating machinery, has demonstrated effectiveness in various studies. A comparative analysis, comparing HPVPA with other diagnostic techniques, becomes instrumental in evaluating its performance in fault detection and diagnosis in induction motors, thereby validating its efficacy and highlighting potential advantages over alternative methods (Allal & *al.*, 2019).

The Park–Hilbert ($PVSM_{P\text{-}H}$) method utilizes the Hilbert transform to acquire complex voltage and current components, extracting spatial information for fault diagnosis in stator windings. Advanced diagnostic techniques like $PVSM_{P\text{-}H}$ contribute to early fault detection in induction motors, preventing the escalation of more severe issues (Sahraoui *et al.*, 2014). Similarly, the Park's Vector Product Approach (PVPA) utilizes Park's vector transformation for obtaining complex voltage and current components in stator and rotor windings. This method calculates the vector product between stator and rotor currents, providing a diagnostic index for early fault detection (Allal & Chetate, 2016).

Researchers analyze various harmonics, such as time harmonics (TH), space harmonics (SH), rotor slot harmonics (RSH), rotor bar fault harmonics (RBFH), and eccentricity fault harmonics (EFH), comparing different diagnostic techniques. Evaluation metrics include sensitivity, specificity, accuracy, and false positive rate. Comparative studies in induction motor fault diagnosis are integral, aiding in the identification of the most effective techniques (Allal & *al.*, 2020).

A study emphasizing the advantages of using residual values for fault detection discusses their ability to identify subtle deviations from normal operating conditions, showcasing effectiveness through comparison with other diagnostic techniques. Utilizing residual values of various harmonics represents a significant advancement in induction motor fault diagnosis, allowing for more sensitive and accurate fault detection (Allal & *al.*, 2021).

This study aims to identify the most sensitive harmonic for detecting stator faults in induction motors through a comparative analysis of four harmonics, potentially including time harmonics (TH), space harmonics (SH), rotor slot harmonics (RSH), and rotor bar fault harmonics (RBFH). The findings have the potential to contribute significantly to the field of induction motor fault diagnosis, enhancing reliability and performance in diverse industrial applications.

2. Methodology

2.1 Harmonics of the induction machines stator current

The air gap field of an Induction Motor (IM) exhibits various discrete space harmonics when subjected to sinusoidal voltage. The subsequent analysis operates under the assumption that these harmonics in the air gap flux result from the interaction between harmonic Magnetomotive Force (MMF) waves and the presence of an air gap. In this context, the focus is specifically on harmonics originating from rotor slotting, referred to as Rotor Slot Harmonics (RSHs). Studies indicate that Rotor Slot Harmonics (RSHs) manifest in the stator line current of a well-functioning machine at frequencies delineated by established frequency values (Boucherma *et al.*, 2006).

$$f_{RSH}(k,s)=\left|\left(1\pm\frac{kN_r}{p}(1-s)\right)f_s\right|_{k=1,2,3,\ldots} \tag{1}$$

$$G=\left\{\left(\left(\frac{kN_r}{p}\pm 1\right)_{k=1,2,3,..}\right)\cap(6\nu\pm 1)_{\nu=1,2,3,..}\right\} \tag{2}$$

k: positive integer, “1”: fundamental harmonic, s: slip, N_r: rotor slot number, p: pole pairs number, and f_s: fundamental supply frequency.

A balanced voltage system powering a stator winding consisting of three identical coils is implied in this statement in regards to a three-phase induction motor, it is important to identify only the currents produced when the harmonic order is odd and not a multiple of three. The only RSH that can be detected is one whose order falls under one of the following settings (Boucherma *et al.*, 2006).

$$G=\left\{\left(\left(\frac{kN_r}{p}\pm 1\right)_{k=1,2,3,..}\right)\cap(6\nu\pm 1)_{\nu=1,2,3,..}\right\} \tag{2}$$

Where: ν Positive integer and G: harmonics detected set.

In practical scenarios, it is not unusual to encounter different levels of statoric imbalance in induction motors. This imbalance can originate from various factors, including irregularities in voltage supply, residual asymmetry in stator windings, or problems with neutral connections. As a consequence of these factors, all harmonics, including those with multiple orders of three, can be present in the current spectrum.

In a properly operating induction motor with a squirrel cage rotor, the stator current typically consists of two distinct sets of harmonics:

- Time Harmonics (THs) series of frequency (Boucherma *et al.*, 2006).

$$f_{TH}(h) = hf_s \quad \text{or} \quad TH = hf_s \tag{3}$$

- Rotor slots (RSHs) harmonics series of frequency (Boucherma *et al.*, 2006).

$$f_{RSH}(h,k,s) = \left| \left(h \pm \frac{k.N_r}{p}(1-s) \right) f_s \right| \quad \text{or} \quad S^{\pm} = \left| (h f_s \pm k.N_r f_r) \right| \tag{4}$$

Where, h is the time harmonic order, h=1,3,5, and k = 1,2,3,4, ….

There may be additional harmonics present in the stator current of an induction motor, including rotor bar fault harmonics (RBFHs) and eccentricity fault harmonics (EFHs), as mentioned in the question. Harmonics can function as valuable diagnostic tools for identifying and pinpointing motor faults and design deficiencies, as they frequently underlie these issues. In a properly functioning induction motor with a squirrel cage rotor, there are two more sets of harmonics present in the stator current:

- Series of Rotor Bar Fault Harmonics (RBFHs) of Frequency (Allal & Chetate, 2019).

$$f_{RBFH}(h,k,s) = \left| (h \pm 2.ks) f_s \right| \quad \text{or} \quad R^{\pm} = \left| (h \pm 2.ks) f_s \right| \tag{5}$$

- Series of Eccentricity Fault Harmonics (EFHs) of Various Frequencies (Abdelhak *et al.*, 2022; Allal & Chetate, 2019; Boucherma *et al.*, 2006; Devanneaux *et al.*, 2003; Năvrăpescu *et al.*, 2010; Saad *et al.*, 2014).

$$f_{EFH}(h,k,s) = \left| (h \pm \frac{k}{p}(1-s)) f_s \right| \quad \text{or} \quad E^{\pm} = \left| (h f_s \pm k f_r) \right| \tag{6}$$

$f_r = \left(\frac{1}{p}(1-s).f_s \right)$ f_r = 24 Hz, it is the rotation frequency as shown in Table 1.

2.2 Eccentricity Fault Harmonics (EFHs) series of Various Frequencies

A phase currents are the subject of the subsequent analysis. The fundamental and all current harmonics serve as the foundation for the mathematical calculations in this case. Which is why, in a perfect scenario, Abdelhak *et al.*, (2022), Allal & Chetate, (2019), Boucherma *et al.*, (2006); Devanneaux *et al.*, (2003), Năvrăpescu *et al.*, (2010) and Saad *et al.*, (2014) provides the current value at a specific moment in time flowing through the stator phase A.

$$i_{sa}(t)_{\text{healthy}} = \hat{I}_F \cos(2\pi f_s t) \tag{7}$$

Equations (1) - (6) encompass the summation of harmonics. $\hat{I}_F$ Denoting the peak current of the fundamental component (or the time harmonic with a value of 1) of the phase supply, this equation is derived from (Allal & Chetate, 2019).

$$i_{sa}(t)_{\text{healthy}} = \sum_{h=1}^{n} \left[\hat{I}_{TH_h} \cos(2\pi TH_h\, t) + \hat{I}_{S_{h,k}^{\pm}} \cos(2\pi S_h^{\pm}\, t) + \sum_{k=1}^{m} \left[\hat{I}_{R_{h,k}^{\pm}} \cos(2\pi R_{h,k}^{\pm}\, t) + \hat{I}_{E_{h,k}^{\pm}} \cos(2\pi E_{h,k}^{\pm}\, t) \right] \right] \tag{8}$$

$$i_{sa}(t)_{\text{faulty}} = \sum_{h=1}^{n}\left[\hat{I}'_{TH_h}\cos\left(2\pi TH_h\ t\right)+\hat{I}'_{S_{h,k}^{\pm}}\cos\left(2\pi S_h^{\pm}\ t\right)+\sum_{k=1}^{m}\left[\hat{I}'_{R_{h,k}^{\pm}}\cos\left(2\pi R_{h,k}^{\pm}\ t\right)+\hat{I}'_{E_{h,k}^{\pm}}\cos\left(2\pi E_{h,k}^{\pm}\ t\right)\right]\right] \quad (9)$$

Where $\hat{I}_{TH_h}$, $\hat{I}_{S_{h,k}^{\pm}}$, $\hat{I}_{R_{h,k}^{\pm}}$, and $\hat{I}_{E_{h,k}^{\pm}}$ The variables m=1,3,5,7,7,9,… n=1,2,3,4,…, and t correspond to real-time measurements in seconds. The equation represents the maximum current in amperes for Time Harmonics (TH), Rotor Slot Harmonics (RSH), Rotor Bar Fault Harmonics (RBFH), and Eccentricity Fault Harmonics (EFH), respectively, under healthy functioning conditions, as illustrated in Table 2, Figure. 2, and Figure. 3. In the context of this study, slip exhibited only a slight increase during failure. Consequently, the following equation for the stator current was derived in the case of stator or rotor faults:

$(s'\approx s)$ but $(s'\neq s)$,with $\hat{I}'_{TH_h}\neq\hat{I}_{TH_h}$, $\hat{I}'_{S_{h,k}^{\pm}}\neq\hat{I}_{S_{h,k}^{\pm}}$, $\hat{I}'_{R_{h,k}^{\pm}}\neq\hat{I}_{R_{h,k}^{\pm}}$ and $\hat{I}'_{E_{h,k}^{\pm}}\neq\hat{I}_{E_{h,k}^{\pm}}$

Here, $\hat{I}'_{TH_h}$, $\hat{I}'_{S_{h,k}^{\pm}}$, $\hat{I}'_{R_{h,k}^{\pm}}$, and $\hat{I}'_{E_{h,k}^{\pm}}$ In the case of a fault, the supply phase maximum current for Time Harmonics (TH), Rotor Slot Harmonics (RSH), Rotor Bar Fault Harmonics (RBFH), and Eccentricity Fault Harmonics (EFH) is represented as follows. Here, s denotes the slip in the case of healthy functioning, s' in the case of a fault, and $f'_r=\left(\frac{1}{p}.(1-s')f_s\right)$. In the case of a fault, f'_r represents the rotation frequency.

3. Results analysis

3.1 Experimental investigation

The approach for assessing harmonics underwent testing through experimental experiments conducted on three electric motors. The outcomes of these experiments are detailed in the subsequent sections 3.2 sample frequency of 10,000 Hz and an acquisition time of 10 seconds were utilized, yielding a total of 100,000 samples. The frequency resolution was determined using Eq. (10), which involves dividing the sampling frequency by the number of samples.

$$\Delta f=\frac{f_e}{f_e.t_a}=0.1Hz \quad (10)$$

3.2 Experiment

The experimental setup comprises an 11kW Induction Motor (IM) motor (3), a DC generator (1) linked to a variable resistive load through a mechanical coupling to ensure speed synchronization, as depicted in Figure 1. The load can be adjusted by altering the overall resistance value using switches, thereby converting the drawn current into thermal energy. The system is interfaced with a Rheostat for limiting short circuit current (2) and features a current sensor (4). The resulting data is recorded by a digital oscilloscope (Tektronix DPO 4039) (5) and stored on a flash disk in the form of matrix tables containing current data for the three phases and an acquisition time of 10 seconds. Subsequently, the data undergoes processing using Matlab software to obtain the Fast Fourier Transform (FFT) of the stator current, enabling the visualization of different harmonics for subsequent analysis. Table 1 provides a summary of the characteristics of the electric motor employed in the experiment.

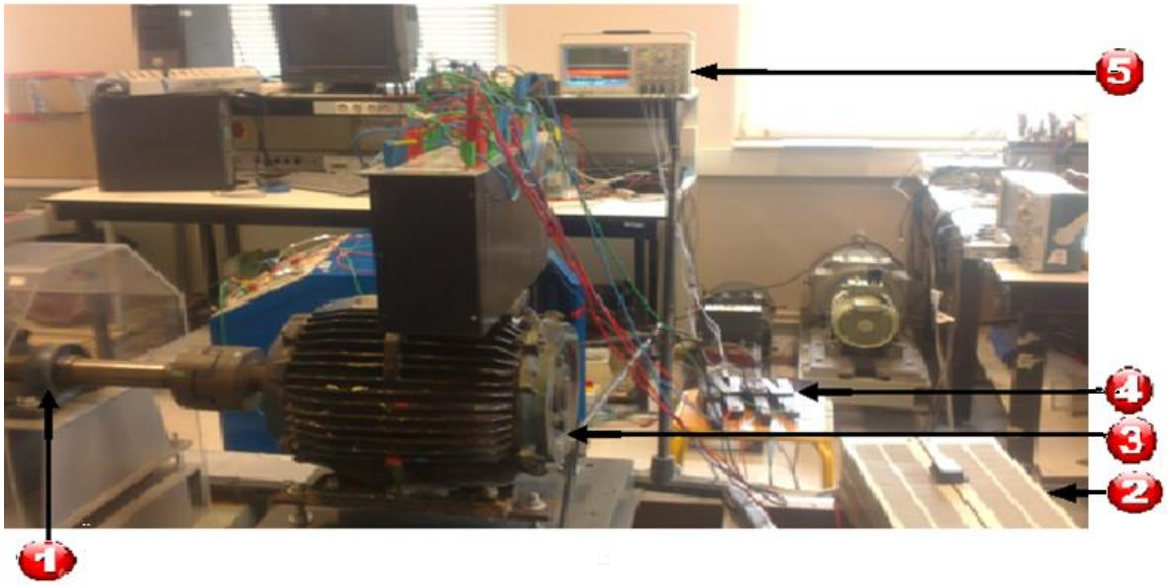

Figure 1. Collecting data for stator current signals (Induction Motor).

Table 1. Induction motor specifications.

Specification	Induction motor (IM)
Rated Power	11 kW
Input voltage	400 V
Full load current	21.5 A
Supply frequency	50 Hz
Rotation frequency	24 Hz
Number of poles	4
Number of rotor bars	32
Full load speed	1440 rpm

Table 2 displays the characteristic frequencies of various harmonics. We have specifically chosen three harmonics with the most sensitive frequency range between 0-100 Hz, highlighted in blue on the graphs. Additionally, we have documented the amplitude values of these harmonics during the operation of a healthy motor under low and full load conditions, represented in red on Figures 2 and 3.

Within this range, we can visualize only:

- The Time Harmonic (TH) with h=1 and a characteristic frequency of 50 Hz. This frequency remains constant regardless of slip, indicating independence from load variations (whether operating at low load or full load). Series of Rotor Bar Fault Harmonics RBFH whose characteristic frequencies can be visualized in this range with (h=1 and k=2),
- A series of Eccentricity Fault Harmonics (EFH) with characteristic frequencies that can be observed in this range, specifically with (h=1 and k=1).

Table 1. Sensitivity of various harmonics to an inter-turn short circuit of 12%.

Harmonic Types	Characteristic frequency (Hz)	Full load		Low load	
		Healthy stator	Faulty stator	Healthy stator	Faulty stator
		$s = 0.012$ Amplitude (dB) / Frequency (Hz)	$s = 0.04$ Amplitude (dB) / Frequency (Hz)	$s = 0.012$ Amplitude (dB) / Frequency (Hz)	$s = 0.04$ Amplitude (dB) / Frequency (Hz)
TH $h = 1$	f_s	**26**.65 / **50**	28.3/50	19.49/50	23.2/50
RSH $h = 15,$ $h = 17$	$RSH- = \lvert(15f_s + N_r f_r)\rvert$	-32.34/18.7	-39.26/18.2	-18.87/25.3	-17.01/25.3
	$RSH+ = \lvert(17f_s - N_r f_r)\rvert$	-31.74/81.3	-34.9/81.8	-20.05/74.7	-18.85/74.7
RBFH	$RBFH- = \lvert(1-2s)f_s\rvert$	-23.28/46.1	-24.58/46	-37.71/48.8	-35.69/48.8
	$RBFH+ = \lvert(1+2s)f_s\rvert$	-35.08/53.9	-33.94/54	-39.73/51.2	-42.32/51.3
EFH $h = 1$	$EFH- = \lvert(f_s - f_r)\rvert$	-32/26	-37.95/26	-27.46/40.3	-42.26/40
	$EFH+ = \lvert(f_s + f_r)\rvert$	32.52/74	29.31/74	33.5/50.7	37.64/60

3.3 Analysis of FFT Spectrum under Low and Full Load

To analyze the stator current of the motor, the initial step involves determining the values of slip, which are contingent on the load. Once slip is established, the characteristic frequencies of each harmonic type can be calculated using general formulas outlined in detail in Figure 2. The position of each harmonic on the abscissa axis can then be readily determined through a straightforward mathematical calculation. Upon identifying the frequencies of the harmonics, the amplitudes of each harmonic can be assessed. It is crucial to note that the amplitudes of different harmonic types may exhibit variations depending on whether the motor is operating in a healthy state or with a stator fault. The disparity in amplitude values between healthy and faulty operation constitutes the sensitivity of the harmonic, as illustrated in Figure 2 and Figure 3.

To pinpoint the most sensitive harmonic with the highest amplitude values, it is necessary to calculate the average value of the sensitivity at low load and full load. This process facilitates the detection of the specific harmonic most affected by the stator fault, serving as a diagnostic tool to identify the location and severity of the fault. In essence, this approach enables effective condition monitoring and fault diagnosis of the motor.

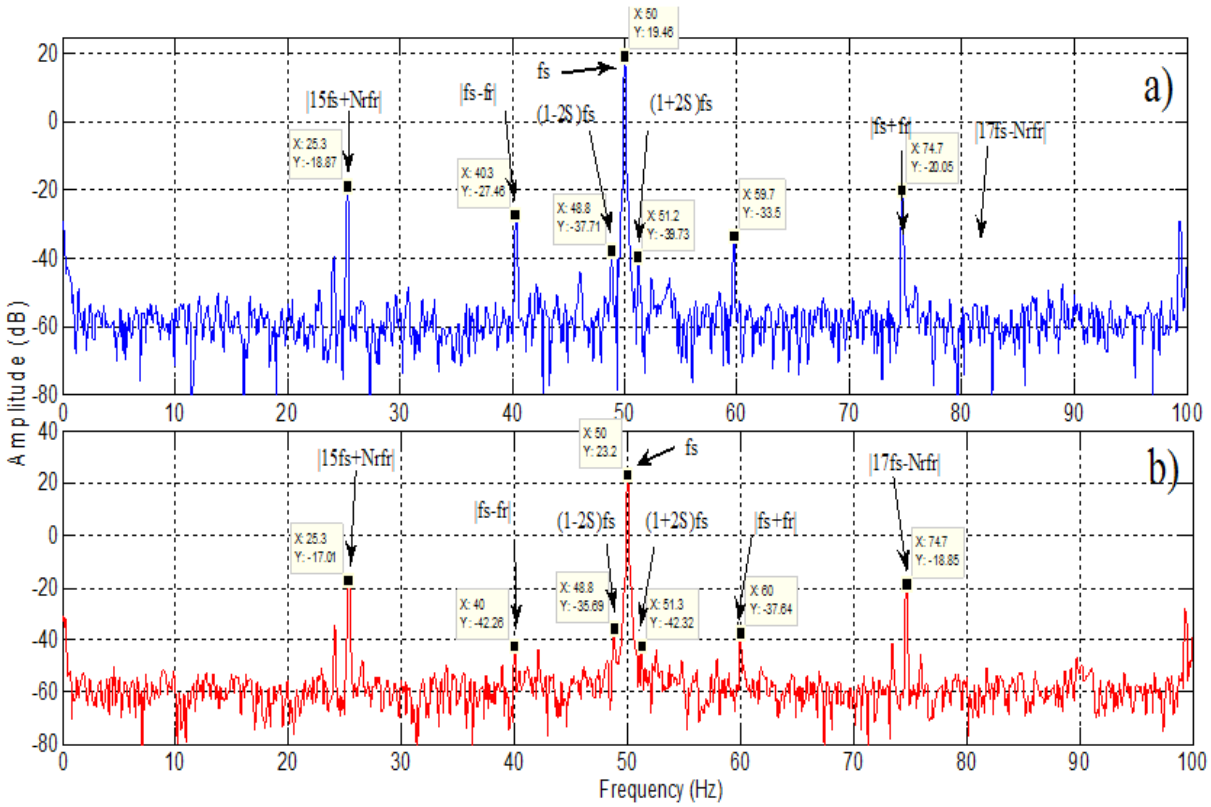

Figure 2. FFT spectrum for low load: (a) Healthy IM, and (b) faulty IM with 12 % of inter turn short circuit in phase A.

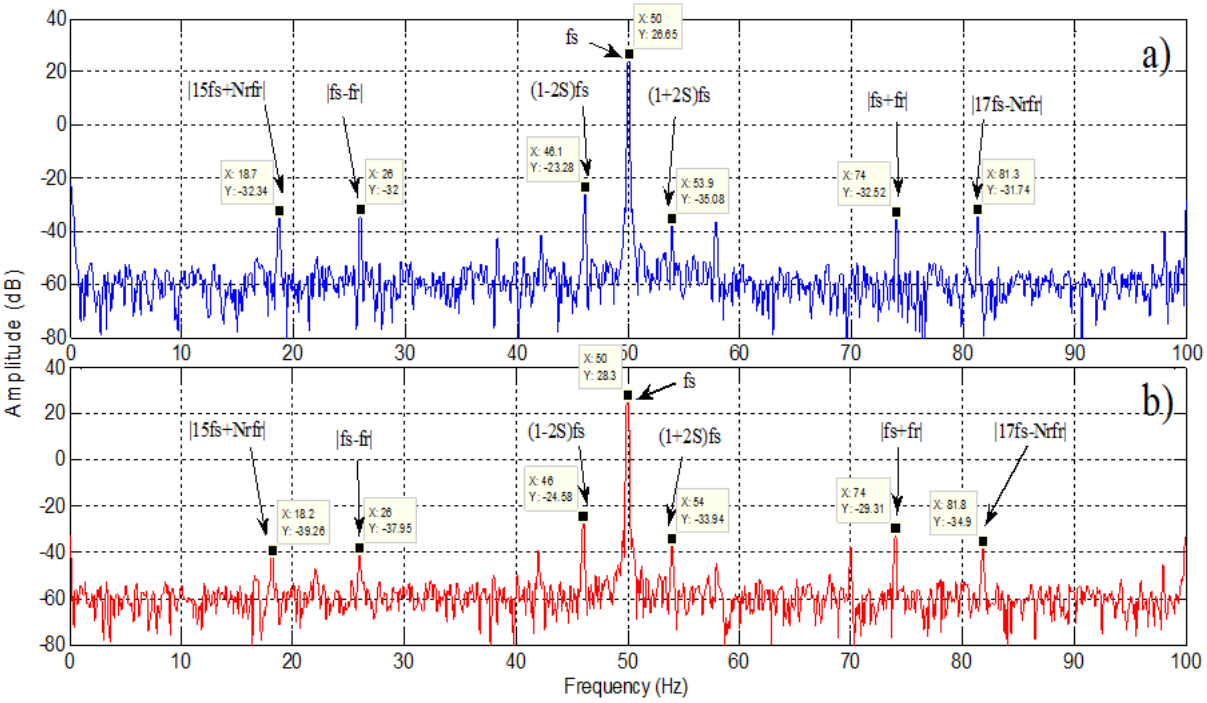

Figure 3. FFT spectrum for full load: (a) Healthy IM, and (b) faulty IM with 12 % of inter turn short circuit in phase A.

3.4 Calculation of the average sensitivity amplitude

The amplitude of the average sensitivity is calculated as the average difference between the amplitudes of the healthy operating regime and the operating regime with a stator fault, under both full load and low load conditions.

$$S(f)\Big|_A = \frac{\left[\left(A(f)\Big|_F - A(f)\Big|_H\right)_{Full} + \left(A(f)\Big|_F - A(f)\Big|_H\right)_{Low}\right]}{2} \tag{11}$$

$S(f)\Big|_A$ The amplitude of the average sensitivity.

$A(f)\Big|_F$ The harmonics amplitude of the regime with fault.

$A(f)\Big|_H$ The amplitude of the harmonics with healthy regime.

Based on the information presented in Figure 4, it can be observed that the harmonics RSH-, RSH+, RBFH-, RBFH+, and EFH- exhibit a relatively low sensitivity, with negative values. The TH and EFH+ harmonics, on the other hand, show excellent sensitivity (positive sensitivity).
The harmonic of time TH has the highest sensitivity, making it the ideal diagnostic criterion for stator defects.

The stator current signal data for any phase can be obtained using a single Hall Effect current sensor, as demonstrated in Figures 4 and 5. Real-time calculation of linear FFT can be performed from the motor power supply. The digital data of the linear FFT in the healthy condition corresponding to the motor's load, estimated slip, and operating conditions can be collected. A distinction is made between the healthy amplitude of the harmonic over time and its actual amplitude. The spectral sweep identifies two potentials scenarios:
(1) No fault exists if there are no harmonics;
(2) Faults exist, if there are harmonics.
The motor operation in the production line is managed according to the severity of the fault, i.e., whether it needs immediate repair or can be deferred until a scheduled shutdown.

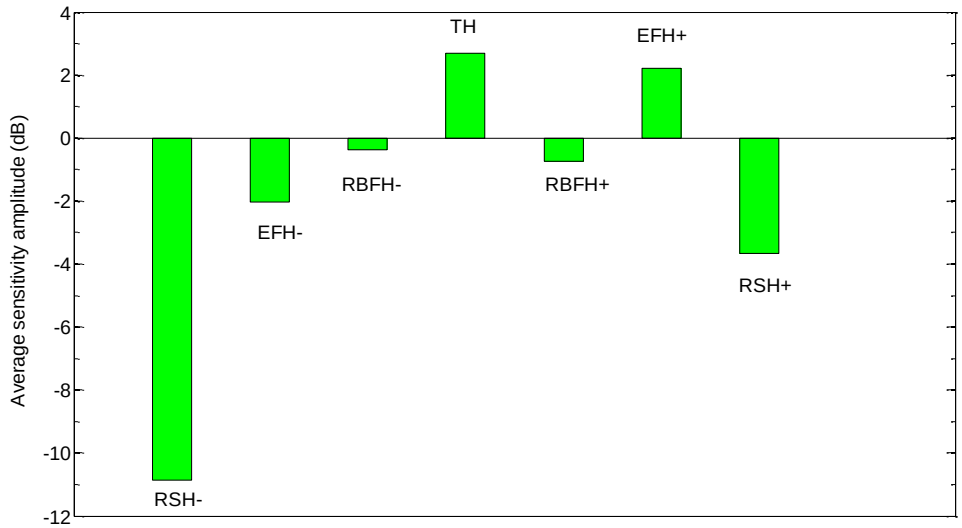

Figure 4. Average sensitivity of the different harmonics.

3.5 Time Harmonic Fault Detection

To automate the monitoring of the system, the flowchart in Figure 5 is followed. The first step involves acquiring the stator phase current data, which is then subjected to FFT analysis in real-time. The next step is to calculate the difference between the real-time amplitude and the amplitude obtained from the database for healthy motor operation under the specific load conditions, determined by the slip value. The residual spectrum is then scanned to check for the presence of residual harmonics, which can indicate the presence of a fault in the motor. The severity of the fault is determined based on the database, and if no residual harmonics are detected, the motor is considered to be in a healthy condition. This automated process streamlines the monitoring of the system and facilitates the early detection of faults in the motor.

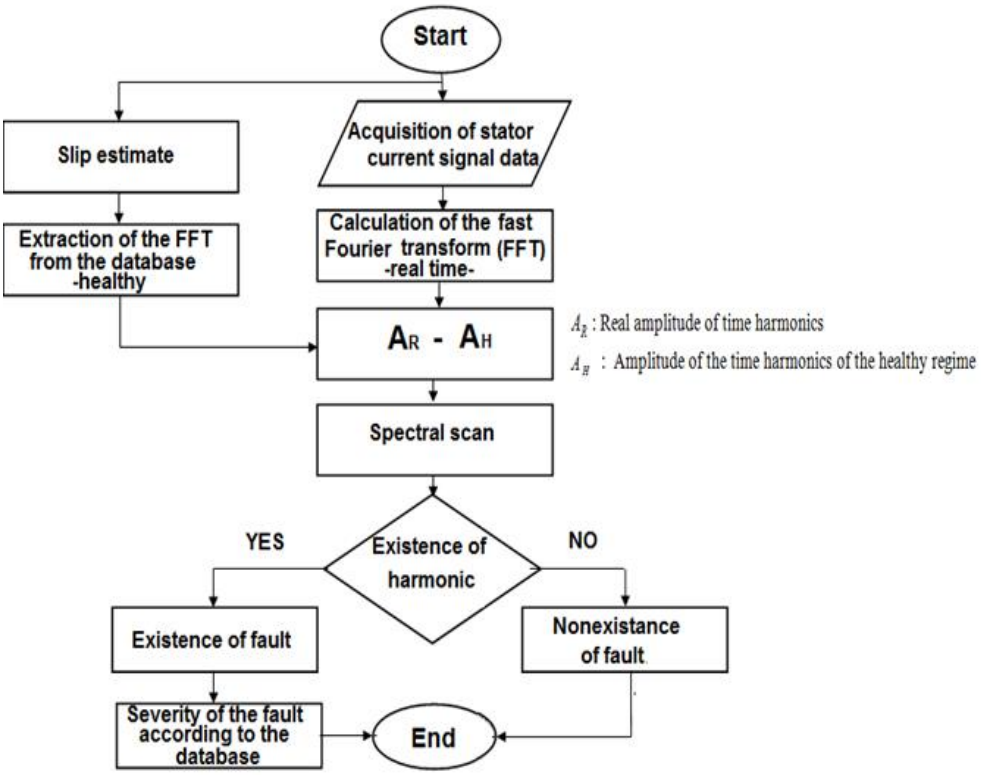

Figure 5. Flowchart for Time Harmonic Fault Detection.

3.5 Discussion

According to Table 2 and Figure 4, the comparison between different harmonics has led to the discovery that the diagnosis of stator faults is more effective with the time harmonic of the fundamental than the other harmonics. It is also promising that real-time monitoring of this harmonic can provide more information on the severity of the fault, allowing for better decision-making in terms of emergency stops versus scheduled stops. Predicting faults through real-time monitoring can definitely reduce unscheduled stops and provide economic advantages, especially in a competitive market where production continuity is crucial. It is important to continue monitoring and analyzing the performance of the system to ensure that it is functioning optimally and to identify any potential faults before they can cause significant damage or downtime.

According to Figure 4, the time harmonic is the most sensitive, and it can be used for programming our automation system. The frequency of the time harmonic remains constant at 50 Hz, regardless of the load variation, making it easy and simple to program the system.

4. Conclusion

The results of this study underscore the significance of signal processing from a single current sensor in power supply lines for analyzing variations in the amplitude of the fundamental time harmonic. This approach facilitates real-time monitoring and diagnosis of stator faults in motors, offering benefits such as continuous machine operation monitoring, and precise detection of fault types based on characteristic frequencies and accurate determination of fault severity by analyzing amplitude differences. Real-time diagnosis not only enables early fault detection but also allows for predictive maintenance, crucial for ensuring production continuity in a competitive market. This proactive approach minimizes unplanned downtime and production losses, leading to substantial cost savings and improved overall system reliability. In summary, leveraging real-time monitoring and diagnosis of harmonic faults provides a strategic advantage, reducing downtime, enhancing system reliability, and optimizing production processes for businesses in a competitive market.

References

A. Allal, B. Chetate. (2019). High sensitivity detection of the stator short-circuit faults in induction motor using Hilbert Park's vector product. *Journal of Fundamental and Applied Sciences, 11*(2), 994-1022.

Abdelhak, G., Sid Ahmed, B., and Djekidel, R. (2022). Fault diagnosis of induction motors rotor using current signature with different signal processing techniques. *Diagnostyka, 23*(2), 2022201. https://doi.org/10.29354/diag/147462

Allal, A., & Chetate, B. (2016). A new and best approach for early detection of rotor and stator faults in induction motors coupled to variable loads. *Front. Energy, 10*(2), 176–191.

Allal, A., Khechekhouche, A. (2022). Diagnosis of induction motor faults using the motor current normalized residual harmonic analysis method. *International Journal of Electrical Power & Energy Systems, 141,* 108219. https://doi.org/10.1016/j.ijepes.2022.108219

Allal, A., Khechekhouche, A., & Driss, Z. (2020). Induction machines diagnosis by the time's harmonics. *International journal of Energetica, 5*(2), 32-36.

Allal, A., Khechekhouche, A., & Driss, Z. (2021). Comparative study of advanced techniques for the diagnosis of induction motors. *Heritage and Sustainable Development, 3*(1), 16-22.

Almounajjed, A., Kumar Sahoo, A., Kant Kumar, Assaf, T. (2022). Fault diagnosis and investigation techniques for induction motor. *International Journal of Ambient Energy, 43*(1), 6341-6361. DOI: 10.1080/01430750.2021.2016483

Alshorman, O., Alshorman, A. (2021). A review of intelligent methods for condition monitoring and fault diagnosis of stator and rotor faults of induction machines. *International Journal of Electrical & Computer Engineering, 11*(4), 2088-8708.

Bilal Djamal Eddine Cherif, Bendiabdellah, A., Tabbakh, M. (2020). An Automatic Diagnosis of an Inverter IGBT Open-Circuit Fault Based on HHT-ANN. *Electric Power Components and Systems, 48*, 589-602. DOI: 10.1080/15325008.2020.1793835

Cherif, H., Benakcha, A., Khechekhouche, A., Menace, A., Panchal, A. (2020). Experimental Diagnosis of inter-turns stator fault and unbalanced voltage supply in induction motor using

MCSA and DWT-SF. *Periodicals of Engineering and Natural Sciences, 4*(3). https://dx.doi.org/10.21533/pen.v8i3.1058

Defdaf, M., Berrabah, F., Chebabhi, A., Cherif, B. D. E. (2021). A new transform discrete wavelet technique based on artificial neural network for induction motor broken rotor bar faults diagnosis. *International Transactions on Electrical Energy Systems, 31*(4), e12807.

Gangsar, P., Tiwari, R. (2020). Signal based condition monitoring techniques for fault detection and diagnosis of induction motors: A state-of-the-art review. *Mechanical Systems and Signal Processing, 144*, 106908.

Glowacz, W., Glowacz, Z., Kozik, J. (2018). Early fault diagnosis of bearing and stator faults of the single-phase induction motor using acoustic signals. *Measurement, 113*, 1-9.

Gyftakis, K. N., Marques Cardoso, A. J., Antonino-Daviu, J. A. (2017). Introducing the Filtered Park's and Filtered Extended Park's Vector Approach to detect broken rotor bars in induction motors independently from the rotor slots number. *Mechanical Systems and Signal Processing, 93*, 30-50.

K. Saad and G. Mirzaeva. (2014). Fault diagnosis of induction motors by space harmonics analysis of the main air gap flux. In *International Conference on Electrical Machines (ICEM)*, Berlin, Germany, 2014, pp. 1608-1613. DOI: 10.1109/ICELMACH.2014.6960397

M. Sahraoui, A. Ghoggal, S. Guedidi, et al. (2014). Detection of inter-turn short-circuit in induction motors using Park–Hilbert method. *International Journal of System Assurance Engineering and Management, 5*(3), 337-351. DOI: 10.1007/s13198-013-0173-6

Mabrouk, A. E., Zouzou, S. E., Khelif, S., Ghoggal, A. (2017). On-line fault diagnostics in operating three-phase induction motors by the active and reactive currents. *Int J Syst Assur Eng Manag, 8*(1), 160–168.

Mohamed Boucherma, M. Y. Kaikaa, A. Khezzar. (2006). Park model of squirrel cage induction machine including space harmonics effects. *Journal of Electrical Engineering, 57*(4), 193-199.

Sapena-Bano, A., Martinez-Roman, J., Puche-Panadero, R., Pineda-Sanchez, M., Perez-Cruz, J., Riera-Guasp, M. (2020). Induction machine model with space harmonics for the diagnosis of rotor eccentricity, based on the convolution theorem. *International Journal of Electrical Power & Energy Systems, 117*, 105625.

Sapena-Bano, A., Martinez-Roman, J., Puche-Panadero, R., Pineda-Sanchez, M., Perez-Cruz, J., Riera-Guasp, M. (2018). Induction machine model with space harmonics for fault diagnosis based on the convolution theorem. *International Journal of Electrical Power & Energy Systems, 100*, 463-481.

Senthil Kumar, R., Gerald Christopher Raj, I., Suresh, K.P., Leninpugalhanthi, P., Suresh, M., Panchal, H., Meenakumari, R., Kumar Sadasivuni K. (2022). A method for broken bar fault diagnosis in three-phase induction motor drive system using Artificial Neural Networks. *International Journal of Ambient Energy, 43*(1), 5138-5144. DOI: 10.1080/01430750.2021.1934117

Tian, L., Hu, B., Cao, X., Zhang, H., Yu, Q. (2022). Multiple open-circuit fault diagnosis of three-phase rectifier based on current data reconstruction. *International Journal of Electronics*. DOI: 10.1080/00207217.2022.2068669

V. Devanneaux, B. Dagues, J. Faucher, G. Barakat. (2003). An accurate model of squirrel cage induction machines under stator faults. *Mathematics and Computers in Simulation, 63*(3-4), 377–391.

Valentin Năvrăpescu, M. Popescu , A-I. Chirilă. I-D.Deaconu, C. Ghită. (2010). Computation methods for space harmonic effects on single-phase induction motor performance. *Rev. Roum. Sci. Techn. – Électrotechn. et Énerg.*, *55*(3), 278–288.

Verucchi, C., Bossio, J., Bossio, G., Acosta, G. (2016). Misalignment detection in induction motors with flexible coupling by means of estimated torque analysis and MCSA. *Mechanical Systems and Signal Processing*, *80*, 570-581.